Printed in U.S.A.

72-GT-31

an ASME publication



$3.00 PER COPY
$1.00 TO ASME MEMBERS

# Computation of Shocked Flows in Compressor Cascades[1]

S. GOPALAKRISHNAN

Development Engineer
Assoc. Mem. ASME

R. BOZZOLA

Chief, Aerodynamic Analysis

Avco Lycoming Div.
Stratford, Conn.

A numerical technique is presented for the calculation of shocked flows in compressor cascades. The problem is posed in the time-dependent form and the asymptotic solution at large times provides the solution of the steady physical problem. The solutions exhibit the formation and movement of shocks as the static pressure ratio across the cascade is varied. The resulting inlet and outlet angles and total pressure loss are also shown.

**Contributed by the Gas Turbine Division of The American Society of Mechanical Engineers for presentation at the Gas Turbine and Fluids Engineering Conference & Products Show, San Francisco, Calif., March 26-30, 1972. Manuscript received at ASME Headquarters, December 8, 1971.**

**Copies will be available until January 1, 1973.**

[1]**This work was accomplished under sponsorship by the U.S. Army Aviation Systems Command.**

THE AMERICAN SOCIETY OF MECHANICAL ENGINEERS, UNITED ENGINEERING CENTER, 345 EAST 47th STREET, NEW YORK, N.Y. 10017

# Computation of Shocked Flows in Compressor Cascades

S. GOPALAKRISHNAN R. BOZZOLA

## INTRODUCTION

Many modern axial flow compressors are designed to be "transonic"; i.e., the relative flow at the inlet of the compressor varies from subsonic at the hub to supersonic at the tip. The exit relative flow is often completely subsonic. The flow at the tip decelerates from supersonic to subsonic through a normal shock. When the exit relative flow is supersonic, the deceleration is achieved through a system of oblique shocks. In the design of such compressors, it is important to know the position and orientation of the shocks in order to estimate the losses and the mass flow through the machine.

Even when the blade element flow is assumed to be two-dimensional, the computation of the tip section is very complicated when normal shocks form. A purely supersonic flow can be calculated by the method of characteristics, and a purely subsonic flow, by the relaxation technique. But a mixed supersonic-subsonic flow with shocks remained intractable until recently.

The advent of the tim-dependent finite difference technique, along with modern high-speed computers, has provided a powerful tool for such mixed problems. An application of this technique to turbomachinery cascades is presented in reference (1).[2] The basic idea of this method is to convert the steady problem into an unsteady one. thereby making the flow equations have a hyperbolic character whether or not the flow is supersonic. Since the character of the flow equations is the same everywhere, a single mathematical technique can be used at all points. The technique usually takes the form of representing the differential equations in terms of finite difference equations and solving the resulting equations algebraically. The concepts of stability and accuracy associated with such finite difference techniques are analyzed in reference (2).

[2] Underlined numbers in parentheses designate References at end of paper.

## NOMENCLATURE

$a$ = local speed of sound
$\mathbf{A}$ = Jacobian matrix of $\vec{F}$ with respect to $\vec{U}$
$b$ = height of lower wall above datum line
$E$ = total internal energy per unit volume
$f$ = factor used in equation (6)
$\vec{F}$ = column vector defined in equation (2), and (7)
$F_t$ = tangential force per unit span
$g$ = eigen value of matrix G
$\vec{G}$ = column vector defined in equation (2)
$h$ = height of upper wall above datum line
$L$ = a characteristic length dimension
$m$ = axial momentum per unit volume
$M$ = Mach number
$p$ = static pressure
$P_T$ = total pressure
$Q$ = mass flow
$Re$ = Reynolds number
$t$ = blade pitch
$\vec{U}$ = column vector defined in equation (7)
$u,v$ = axial and tangential velocity components
$\vec{W}$ = column vector defined in equation (2)
$x,y$ = independent space variables
$\beta$ = flow angles
$\gamma$ = ratio of specific heats
$\Delta$ = incremental quantity
$\epsilon$ = shock thickness
$\varphi$ = smoothing factor
$\lambda$ = eigen value of matrix, $\Lambda$
$\Lambda$ = matrix, $\mathbf{A}\Delta t/\Delta x$
$\rho$ = density
$\nu$ = artificial kinematic viscosity

Subscripts

1 = inlet plane
2 = exit plane

Superscripts

$\Lambda$ = non-dimensional variable
* = sonic condition

decreased to about 1.5 depending upon the magnitude of $\varphi$.

## SHOCK COMPUTATION

In the absence of viscosity effects, the shock transition occurs discontinuously. The flow variables on either side of the shock satisfy the Rankine-Hugoniot conditions. In real fluids with small viscosity, this jump in flow variables takes place smoothly, although very rapidly. The idea of Von Neumann and Richtmyer (2) was to introduce an artificial dissipative mechanism, which will produce a smooth transition in the flow variables through the shock. The choice of this artificial viscosity was made such that the smearing of the shock would be independent of the shock strength. The artificial dissipation was introduced in their scheme by means of an artificial viscous pressure proportional to the square of the spatial derivative of the velocity. Examples of such shock calculation can be found in reference (2). Typically, if the artificial viscosity is too small, the shock transition is rapid, but there are unacceptable oscillations behind the shock. By increasing the viscosity, the oscillation can be cut down, but the shock transition is less rapid. An acceptable result can be obtained by suitable choice of the viscosity. In any case, the artificial viscosity is very much larger than the true viscosity.

In the present method, artificial dissipation is introduced by means of the smoothing operator. A linear analysis of the one-dimensional equation of fluid mechanics is carried out in the Appendix and indicates the effect of the smoothing operator on the dissipative properties of the system. The smearing produced on the shock by the smoothing step is a function of the shock strength, a weak shock being smeared much more than a strong shock. However, no decrease in allowable time step size, $\Delta t$, is necessary; whereas for the Von-Neumann Richtmyer viscosity, the allowable $\Delta t$ is reduced significantly (4).

## APPLICATION TO COMPRESSOR CASCADES

In the operation of a compressor rotor with supersonic relative inlet Mach number, but with subsonic axial velocity, it is known (5) that there is a unique incidence associated with the given inlet Mach number as long as the shock is not spilled out. If the flow is not at this incidence, a wave emanates from the rotor and changes the inlet flow angle to the right direction. The exit angle depends upon the blade circulation which, in turn, is fixed by the Kutta condition.

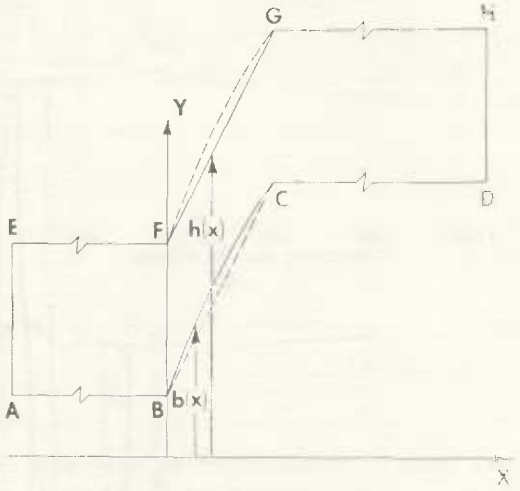


Fig. 1 Compressor cascade geometry

Thus, neither the inlet nor the exit angle are known a priori for the usual transonic compressor operation. The only flow properties that are independently variable are the inlet Mach number and the static pressure ratio. The problem is then to find the entire flow field given the blade geometry, the inlet Mach number, and the static pressure ratio. The inlet and exit angles, as well as the total pressure loss of the cascade, must be computed as part of the solution.

A channel for the flow is defined in Fig. 1. AE and DH are the inlet and exit planes. The lines AB, CD, EF, and GH are imaginary boundaries which the fluid is allowed to cross. The x and y coordinates are suitably transformed to achieve a rectangular computational domain with equal $\Delta x$ and equal $\Delta y$. The initial conditions are arbitrarily assigned as in reference (1). They have no effect on the final solution, but only on the time taken to reach convergence.

The flow variables on the blade surface are computed by a first-order analog of the differential equations using one-sided derivatives. The condition of tangency of the flow to the blade surface is used in place of the tangential momentum equation. The boundaries AB, CD, EF, and GH are computed using the periodicity properties. The inlet angle is allowed to be time-dependent, and computed at every cycle by equating the mass flow at the inlet plane to that of the previous cycle at a plane between the leading and trailing edges. The physical basis for such a technique is that the change in inlet angle produced by the wave system is felt as a change in mass flow. For the computation of the exit angle, the flows on the pressure and suction surfaces are assumed to

Fig. 2 Constant Mach number contours for pressure ratio = 1.64

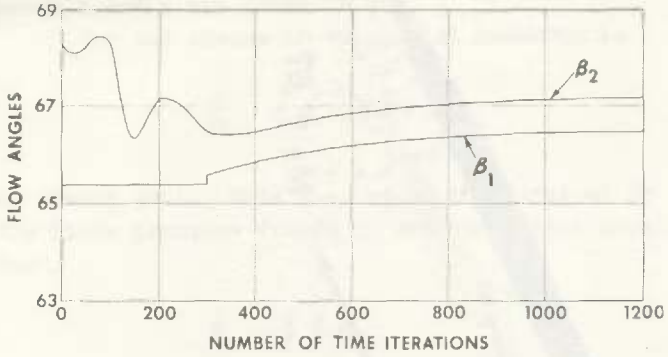


Fig. 3 Approach to convergence of inlet and exit angles

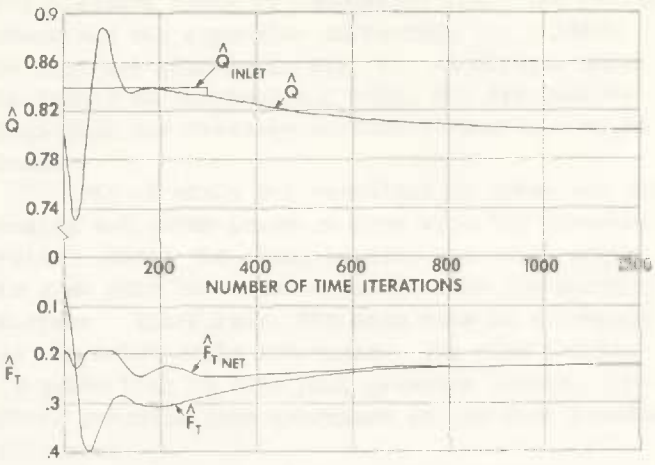


Fig. 4 Approach to convergence of mass flow and tangential momentum

join at the trailing edge, thereby imposing a restriction similar to the Kutta condition.

RESULTS

The method outlined in the foregoing has been applied to the flow through the tip section of a compressor rotor. The change in the streamline radius and the stream filament thickness were ignored, thereby reducing the flow to a two-dimensional one. The inlet relative Mach number is 1.42, and the static pressure ratio is varied from 1.2 to 2.7.

Fig. 2 shows the computed constant Mach number lines for the pressure ratio of 1.64. The computed flow angle is 66.51 and is parallel to the nearly flat inlet region of the suction surface. The pressure side makes a small angle of about 3 deg to this direction, and, hence, an oblique wave forms. This wave is smeared over several mesh spaces for reasons mentioned in the Appendix. This wave interacts with the expansion fan produced on the suction surface resulting in the closure of the Mach number lines on to the pressure surface. At the end of the expansion, the surface Mach number reaches a value of about 1.6, and a strong curved shock is formed. This shock spans the passage width, and the Mach number is reduced to high subsonic values.

The pressure ratio of 1.64 is too small to be obtained by a normal shock with $M_1 = 1.42$ and too big to be obtained by a system of oblique shocks. Hence, the flow adjusts by expanding to low enough pressures and high enough Mach numbers and then going through a strong nearly, normal shock wave. This behavior is analogous to that of the one-dimensional flow in Laval nozzles at low back pressures.

Fig. 2 also shows the variation of total pressure in the transverse direction. Along section A-A, the ratio, $Pt/Pt_1$, is very nearly equal to 1. The oblique shock losses are very small. Along section B-B toward the pressure side, the total pressure drops as the shock is crossed. Along section C-C, total pressure has decreased over the whole width. This shows that the total pressure losses are computed by the method in a manner consistent to shocked flow.

Fig. 3 shows the approach to convergence of the inlet and exit angles with the number of time iterations. The inlet angle is held constant for the first 300 cycles at an initially guessed value. After about 1000 cycles, the two angles have settled down to very nearly their asymptotic values.

Convergence is also checked by plotting the variation of the mass flow at an arbitrary section, as well as the net change in tangential momentum.

The following definitions are employed.

$$\hat{Q}_{inlet} = \text{Mass flow at the inlet plane} = \hat{\rho}_1 \hat{u}_1 \hat{t}_1$$

where the superscript, $\wedge$, refers to non-dimensionalization as follows:

$$\hat{\rho} = \frac{\rho}{\rho_1^*} \quad ; \quad \hat{u} = \frac{u}{a_1^*} \quad ; \quad \hat{v} = \frac{v}{a_1^*} \quad ; \quad \hat{p} = \frac{p}{\gamma p_1^*} \quad ; \quad \hat{t} = \frac{t}{L}$$

where subscript 1 refers to the inlet plane, subscript 2 refers to the exit plane, superscript * refers to the sonic condition, t pitch of the cascade, and L is a characteristic length dimension. At any arbitrary transverse station, the mass flow is:

$$\hat{Q} = \int_{\hat{b}}^{\hat{h}} \hat{\rho}\,\hat{u}\,d\hat{y}$$

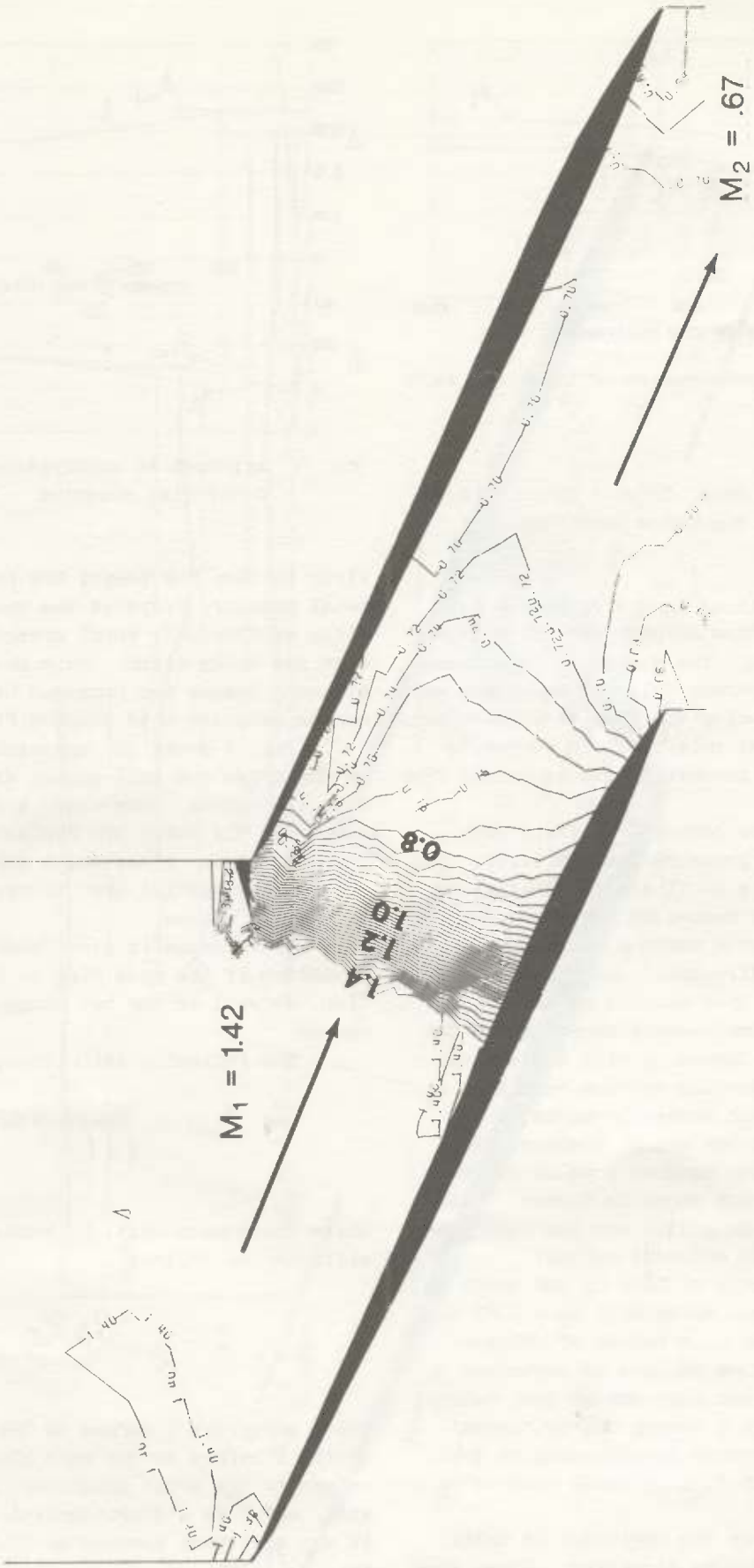


Fig. 5 Constant Mach number contours for pressure ratio = 2.2

where b and h are shown in Fig. 1.

The net change in tangential momentum is

$$\hat{F}_T = \hat{t}\,\hat{\rho}_1\,\hat{u}_1\,(\hat{v}_2 - \hat{v}_1)$$

At steady state, this must equal the integral of the blade pressure forces in the tangential direction.

$$\hat{F}_T = \oint \hat{p}\, d\hat{x}$$

The upper part of Fig. 4 shows the variation of $\hat{Q}_{inlet}$ and $\hat{Q}$ with the number of time iterations. For the first 300 cycles, $\hat{Q}_{inlet}$ is held constant at the given initial value. Later it is allowed to change. By about 1000 cycles, convergence is reached.

The lower part of Fig. 4 shows the variation of $\hat{F}_{T_{net}}$ and $\hat{F}_T$. After the rapid initial oscillations, the variations subside by about 1000 cycles. When the variations in all five variables ($\beta_1, \beta_2, \hat{Q}, \hat{F}_T, \hat{F}_{T_{net}}$) die down to satisfactory levels, convergence is taken to be reached and the solution is taken as the steady-state solution.

It is instructive to consider the effect of back pressure on the cascade operation. With the inlet Mach number held at 1.42, the pressure ratio of the cascade was increased to 2.2. In running this and the next cases, $\Delta t$ was increased somewhat and $\varphi$ decreased to keep the damping given by $\varphi\Delta t$ constant. This resulted in reducing the number of time cycles required for convergence.[3] The Mach number contours for this pressure ratio of 2.2 are shown in Fig. 5. The shock has moved close to the leading edge, and a jump in flow variables nearly equal to that given by the normal shock relations takes place in about 3 mesh spaces. After the shock transition on the suction surface, diffusion takes place due to area change.

Fig. 6 shows the Mach number contours when the pressure ratio is increased to 2.7. The shock is now spilled out. The computed inlet angle is 71.15, and the suction surface is at a positive incidence. As the flow goes around the leading edge, expansion waves are generated and these interact with the extended bow shock. The bow shock gets attenuated in strength and, hence, has only a finite extent.

Fig. 7 shows the Mach number contours when the pressure ratio is reduced to 1.2. The oblique shock and the expansion waves from the suction surface are seen as in Fig. 2. An oblique shock is formed at the trailing edge, but its reflection from the pressure surface is too weak to be seen.

Fig. 8 shows the variation of inlet and exit angles and total pressure loss with the pressure ratio. Until the shock spills, the inlet angle is such that the flow is parallel to the suction surface. Thereafter, the mass flow is decreased as the inlet angle increases. The flow turning is quite high at high back pressure levels. The total pressure loss increases as the back pressure increases.

No attempt has been made to compare these results with experimental data because of the inavailability of detailed two-dimensional compressor cascade data with little shock boundary-layer interaction. However, satisfactory agreement has been indicated with an exact solution for a simple two-dimensional supersonic flow in reference (1).

## CONCLUSIONS

1 The time-dependent finite difference technique is a useful tool for the study of shocked flow in compressor cascades. The position, orientation, and magnitude of the shocks can be easily identified.

2 The method predicts the incidence as a function of the static pressure ratio for cascades having supersonic inlet relative flow.

3 The method also yields information on the inviscid total pressure losses and turning of the cascade.

4 The smoothing operator introduced in equation (5) is an effectve damping device for oscillations generated in the vicinity of the shock.

## ACKNOWLEDGMENT

The authors are deeply grateful to the management of AVCO Lycoming for permission to present this paper.

## APPENDIX

The equations of one-dimensional, unsteady, compressible fluid flow can be written as:

$$\frac{\partial \vec{U}}{\partial t} + \frac{\partial}{\partial x}\vec{F}(\vec{U}) = 0 \qquad (7)$$

where $\vec{U}$ and $\vec{F}(\vec{U})$ are column vectors given by:

[3] With a 34 x 11 grid, the computation time per case is about 10 min. on an IBM 370/155 system.

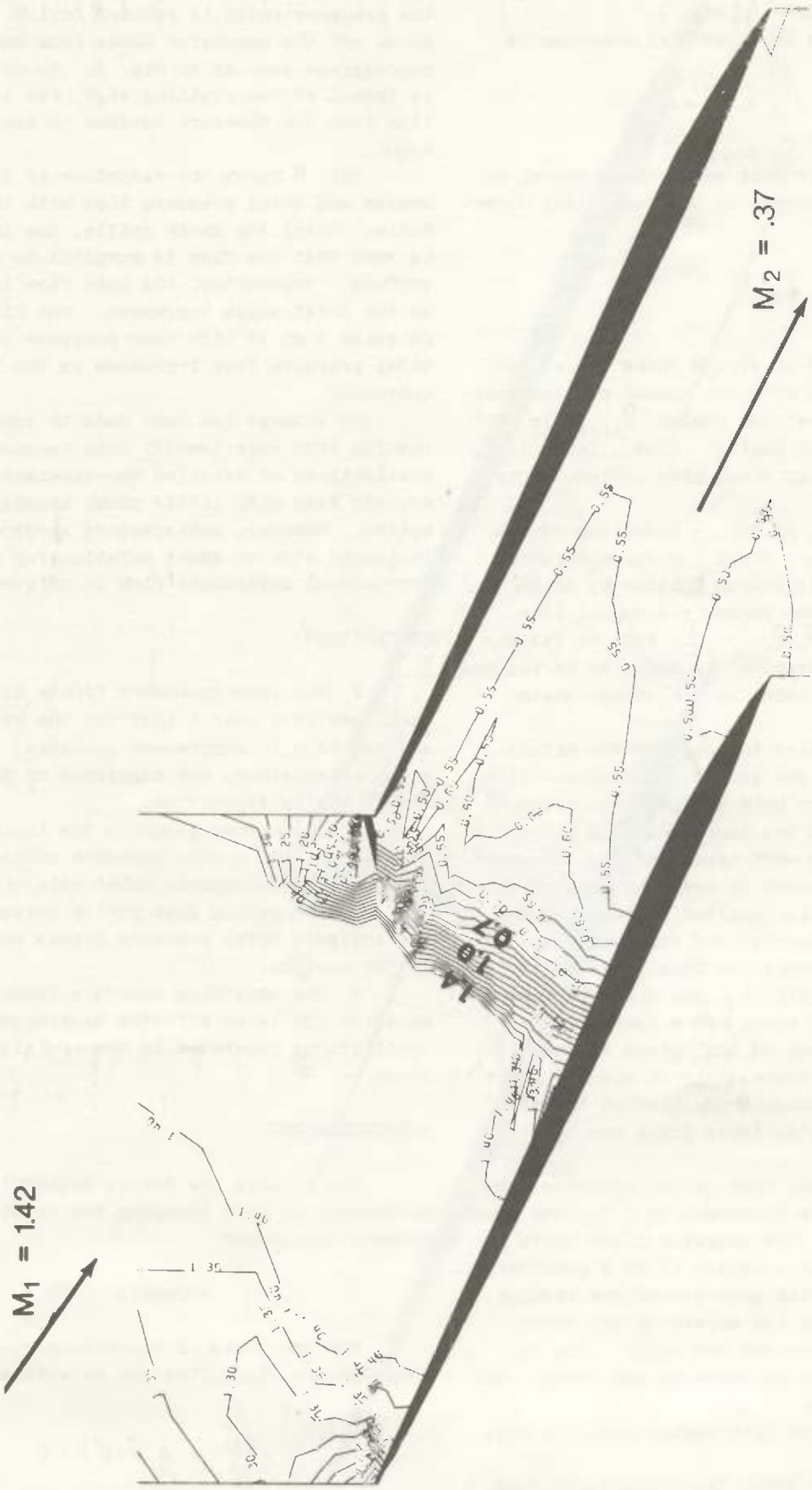


Fig. 6 Constant Mach number contours for pressure ratio = 2.7

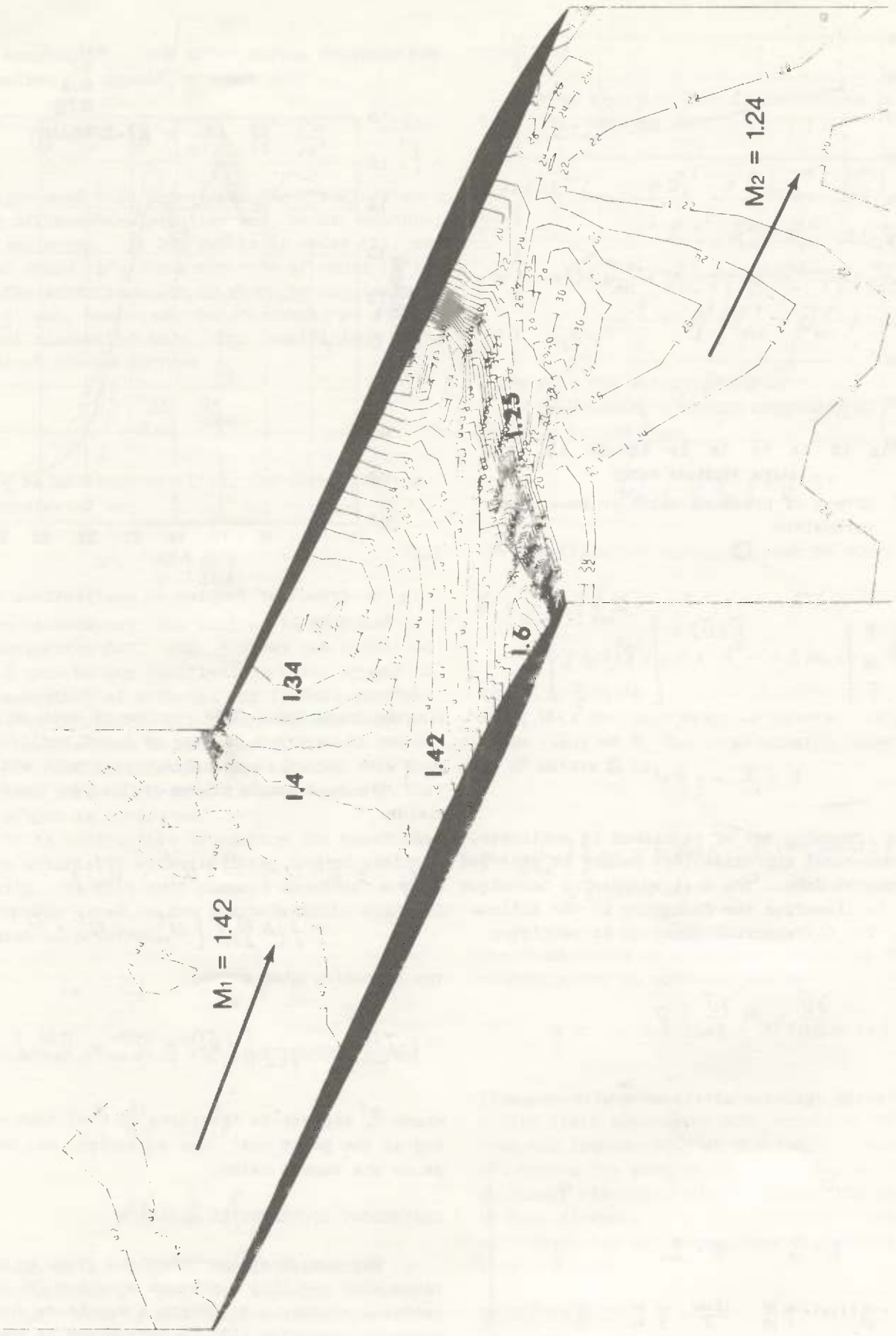


Fig. 7 Constant Mach number contours for pressure ratio = 1.2

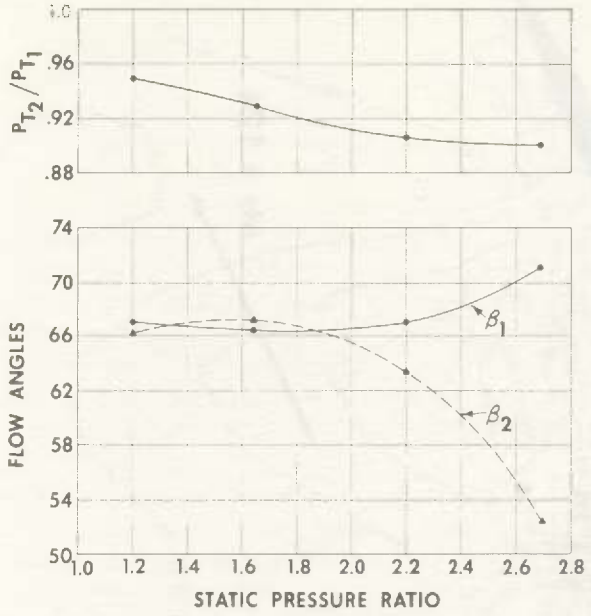


Fig. 8 Effect of pressure ratio on some flow parameters

$$\vec{U} = \begin{bmatrix} \rho \\ m \\ E \end{bmatrix} \qquad \vec{F}(\vec{U}) = \begin{bmatrix} m \\ \frac{m^2}{\rho} + p \\ (E+p)\frac{m}{\rho} \end{bmatrix} \tag{8}$$

$$m = \rho u$$

$$E = \frac{p}{\gamma - 1} + \frac{1}{2}\rho u^2$$

The foregoing set of equations is nonlinear, and its numerical approximations cannot be analyzed in the general form. The most successful technique has been to linearize the foregoing in the following way. The differential equation is rewritten as:

$$\frac{\partial \vec{U}}{\partial t} + A\frac{\partial \vec{U}}{\partial x} = 0 \tag{9}$$

where $A$ is the Jacobian matrix of $\vec{F}$ with respect to $\vec{U}$.

$$A = \begin{bmatrix} 0 & 1 & 0 \\ -\frac{m^2}{\rho^2} + \frac{\partial p}{\partial \rho} & \frac{2m}{\rho} + \frac{\partial p}{\partial m} & \frac{\partial p}{\partial E} \\ -\frac{m}{\rho^2}(E+p) + \frac{m}{\rho}\frac{\partial p}{\partial \rho} & \frac{(E+p)}{\rho} + \frac{m}{\rho}\frac{\partial p}{\partial m} & \frac{m}{\rho}\left(1 + \frac{\partial p}{\partial E}\right) \end{bmatrix}$$

When $A$ is assumed constant, the differential equation is linearized. The results of such an analysis can be expected to give at least qualitative guidance with regard to stability, accuracy, etc.

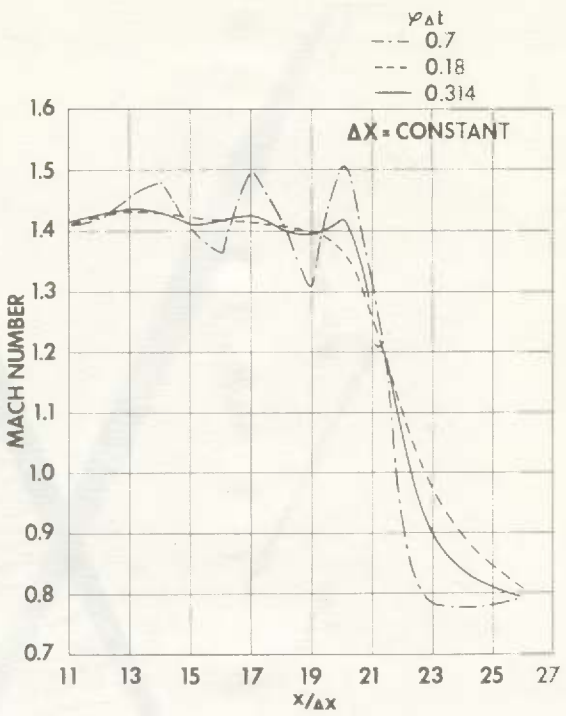


Fig. 9 Effect of damping on oscillations near shock

The MacCormack scheme applied to the set (9) yields:

$$\vec{U}_n^{\ell+1} = \vec{U}_n^{\ell} - \frac{A}{2}\frac{\Delta t}{\Delta x}\left(\vec{U}_{n+1}^{\ell} - \vec{U}_{n-1}^{\ell}\right) + \frac{1}{2}\left(A\frac{\Delta t}{\Delta x}\right)^2\left[\vec{U}_{n+1}^{\ell} - 2\vec{U}_n^{\ell} + \vec{U}_{n-1}^{\ell}\right] \tag{10}$$

The smoothing step gives:

$$\left(\vec{U}_n^{\ell+1}\right)_{sm} = \frac{1}{\varphi+2}\left[\varphi\vec{U}_n^{\ell+1} + \vec{U}_{n-1}^{\ell+1} + \vec{U}_{n+1}^{\ell+1}\right] \tag{11}$$

where $\vec{U}_n^{\ell}$ represents the value of $\vec{U}$ at time $= \ell\Delta t$ and at the point $n\Delta x$. The subscript, sm, represents the smooth value.

## EQUIVALENT DIFFERENTIAL EQUATION

The numerical approximation given by equations (10) and (11) represent equation (9) to a certain accuracy. To obtain a magnitude for this accuracy, equation (10) is introduced in equation (11), and the terms of the latter are expanded using a Taylor Series. The expressions are grou-

cated consistently, and after making repeated use of equation (9) itself, one can get:

$$\frac{\partial \vec{U}}{\partial t} + A \frac{\partial \vec{U}}{\partial x} = \frac{1}{\varphi+2} \frac{\Delta x^2}{\Delta t} \frac{\partial^2 \vec{U}}{\partial x^2} \qquad (12)$$

The right-hand side represents the modification of the differential equation and, hence, constitutes the error. If $\partial^2 \vec{U}/\partial x^2$ is of order (1), and $\varphi$ is of order $(1/\Delta)$, the error is of order $(\Delta^2)$.

The error term can be shown to be dissipative (1) and, hence, may be considered as an "artificial viscosity" term. The "coefficient of viscosity" can be defined

$$\nu = \frac{\Delta x}{\varphi+2} \frac{\Delta x}{\Delta t}$$

Since $\varphi$ is at least of $(1/\Delta)$, the foregoing can be approximated as

$$\nu = \frac{\Delta x}{\varphi} \left(\frac{\Delta x}{\Delta t}\right) \qquad (13)$$

When $\Delta x$ is constant, the damping is produced by the combination $\varphi \Delta t$. Fig. 9 shows the effect of the $\varphi \Delta t$ term on the oscillations which appear in the computation of a shock. $\Delta x$ is held constant, and as $\varphi \Delta t$ increases (i.e., damping dicreases), strong oscillations in Mach number appear. For lower $\varphi \Delta t$, the oscillations are reduced, but the shock gets smeared further. A compromise in the value of $\varphi \Delta t$ is indicated.

It is instructive to compare the magnitude of this artificial viscosity with the physical viscosity. To this end, one may construct a Reynolds number based on the characteristic physical dimension of problem.

$$Re = \frac{u L}{\nu} = u \frac{L}{\Delta x} \varphi \frac{\Delta t}{\Delta x}$$

For transonic flow ($u \approx a$), equation (6) gives

$$\frac{\Delta t}{\Delta x} = \frac{1}{2uf}$$

Hence

$$Re = \frac{L}{\Delta x} \frac{\varphi}{2f}$$

With $\Delta x/L = 0.02$ (a higher resolution is impractical) and $\varphi = 500$, the Reynolds number is about 1000. This is much smaller than the usual Reynolds number for high-speed flow ($\sim 10^6$), and, consequently, the computed shock has considerably larger thickness than would normally be observed.

STABILITY

When equation (10) is introduced in equation (11), one can get:

$$(\varphi+2)(\vec{U}_n^{\ell+1})_{sm} = \varphi \vec{U}_n^{\ell} - \varphi \frac{A}{2}(\vec{U}_{n+1}^{\ell} - \vec{U}_{n-1}^{\ell}) + \varphi \frac{A^2}{2}(\vec{U}_{n+1}^{\ell} - \vec{U}_{n-1}^{\ell} - 2\vec{U}_n^{\ell}) + (1-A^2)(\vec{U}_{n+1}^{\ell} + \vec{U}_{n-1}^{\ell}) + A^2 \vec{U}_n^{\ell} - \frac{A}{2}(\vec{U}_{n+2}^{\ell} - \vec{U}_{n-2}^{\ell}) + \frac{A^2}{2}(\vec{U}_{n+2}^{\ell} + \vec{U}_{n-2}^{\ell})$$

Where $A$ is the matrix, $A(\Delta t/\Delta x)$.

Considering a single component of an assumed solution of the form

$$\vec{U}_n^{\ell} = \sum_m B_m \vec{\xi}^{\ell} e^{imx}$$

the amplification matrix, $G$, can be shown to be:

$$G = \frac{1}{\varphi+2}\left[\left\{ I - iA \sin x - A^2(1-\cos x)\right\}\varphi + (I-A^2)2\cos x + A^2 - iA \sin 2x + A^2 \cos 2x\right]$$

where $I$ is the unit diagonal matrix. If $\lambda$ is an eigen value of $A$, the corresponding eigen value, $g$, of matrix $G$ is

$$g = \frac{1}{\varphi+2}\left[\left\{ 1 - i\lambda \sin x - \lambda^2(1-\cos 2x)\right\}\varphi + (1-\lambda^2)2\cos x + \lambda^2 - i\lambda \sin 2x + \lambda^2 \cos 2x\right]$$

The usual value of $\varphi$ is large enough so that the foregoing may be approximated as

$$g \simeq 1 - i\lambda \sin x - \lambda^2(1-\cos 2x) \qquad (14)$$

It has been shown in reference (2) that the stability limit associated with equation (14) is $\lambda < 1$. Then the introduction of the damping operation does not reduce the permissible $\Delta t$. The Von-Neumann Richtmyer viscosity scheme reduces the allowable $\Delta t$ significantly (2), thus requiring larger number of time cycles for convergence and, hence, higher computer costs.

SHOCK THICKNESS

From equation (12), the momentum equation in the x-direction can be deduced as:

$$\frac{\partial m}{\partial t} + \left[ -\frac{m^2}{\rho^2} + \frac{\partial p}{\partial \rho} \right] \frac{\partial \rho}{\partial x} + \left[ \frac{2m}{\rho} + \frac{\partial p}{\partial m} \right] \frac{\partial m}{\partial x} + \frac{\partial p}{\partial E} \frac{\partial E}{\partial x} = \frac{1}{\varphi+2} \frac{\Delta x^2}{\Delta t} \frac{\partial^2 m}{\partial x^2}$$

This may be simplified to

$$\frac{\partial}{\partial t}(\rho u) + \frac{\partial}{\partial x}(\rho u^2 + p) = \frac{1}{\varphi+2} \frac{\Delta x^2}{\Delta t} \frac{\partial^2 (\rho u)}{\partial x^2} \quad (15)$$

If the continuity equation

$$\frac{\partial \rho}{\partial t} + \frac{\partial}{\partial x}(\rho u) = \frac{1}{\varphi+2} \frac{\Delta x^2}{\Delta t} \frac{\partial^2 \rho}{\partial x^2}$$

is substituted in equation (15), the momentum equation becomes, in the steady state,

$$u \frac{\partial u}{\partial x} + \frac{1}{\rho} \frac{\partial p}{\partial x} = \frac{1}{\varphi+2} \frac{\Delta x^2}{\Delta t} \frac{\partial^2 u}{\partial x^2} \quad (16)$$

This equation has the same form as that for one-dimensional viscous flow through a shock wave (6).

$$u \frac{\partial u}{\partial x} + \frac{1}{\rho} \frac{\partial p}{\partial x} = \bar{\nu} \frac{\partial^2 u}{\partial x^2} \quad (17)$$

where the right-hand side represents the compressive stress due to viscosity effects, and $\bar{\nu}$ is an appropriate coefficient of kinematic viscosity. It is shown in reference (6) that the shock thickness, $\epsilon$ (defined in any reasonable manner), can be expressed as:

$$\epsilon \propto \frac{\bar{\nu}}{\Delta u}$$

where $\Delta u$ is the jump in velocity across the shock wave. Since equations (16) and (17) have the same form, the shock thickness obtained in the computation can be written as:

$$\epsilon \propto \frac{\Delta x^2}{\varphi \Delta t} \frac{1}{\Delta u}$$

replacing $\varphi + 2$ by $\varphi$ for large $\varphi$

Thus large values of $\varphi(\Delta t/\Delta x^2)$ (i.e., little damping) produce narrow shock layers as expected. However the shock thickness depends upon the shock strength. Weak waves are smeared much more than the strong ones. The weak oblique wave at the leading edge in Figs. 2 and 7 is smeared much more than the much stronger wave at the trailing edge.

The Von-Neumann Richtmyer viscosity is tailored to overcome this drawback. The viscous stress in their scheme is proportional to

$$\left( \frac{\partial u}{\partial x} \right)^2$$

and the shock thickness has been shown to be independent of the shock strength (2).

REFERENCES


1 Gopalakrishnan, S. and Bozzola, R., "A Numerical Technique for the Calculation of Transonic Flows in Turbomachinery Cascades," ASME Paper No. 71-GT-42, Gas Turbine Conference and Products Show, Houston, Tex., March 1971.

2 Richtmyer, R. D., and Morton, K. W., Difference Methods for Initial Value Problems, 2nd Edition, Interscience Publishers, New York, 1967.

3 MacCormack, R. W., "The Effect of Viscosity in Hypervelocity Impact Cratering," AIAA Paper No. 69-345, AIAA Hypervelocity Impact Conference, Cincinatti, Ohio, May 1969.

4 Burstein, S. Z., "Numerical Methods in Multi-Dimensional Shocked Flows," AIAA Journal, Vol. 2, No. 12, 1964.

5 "Aerodynamic Properties of Supersonic Compressors," in Hawthorne, W. R., Ed., "Aerodynamics of Turbines and Compressors," Ferri, A., Princeton University Press 1964.

6 Liepmann, H. W., and Roshko, A., Elements of Gas Dynamics, John Wiley and Sons Inc., New York, 1963.